JOURNAL OF MATERIALS SCIENCE **35** (2000) 5661–5665

# The influence of the stress ratio on fatigue crack growth in a cermet

S. ISHIHARA, T. GOSHIMA, Y. YOSHIMOTO, T. SABU
*Department of Mechanical Engineering, Toyama University, Toyama 930-8555, Japan*
*E-mail: ishi@eng.toyama-u.ac.jp*

A. J. McEVILY
*Department of Metallurgy, University of Connecticut, Storrs, CT 06269, USA*

The fatigue crack growth behavior in a cermet was investigated as a function of the stress ratio, $R$. At the higher $K_{max}$ values the fracture path was through the cermet particles as well as through the binder phase. At low growth rates the fracture path was primarily through the binder phase. As a result the fatigue crack growth process, at a growth rate of l0$^{-7}$ m/cycle the rate was influenced by $K_{max}$, and to a lesser extent by the $R$ value, whereas at a growth rate of $10^{-11}$ m/cycle the growth rate depend upon $\Delta K$ as well as the $R$ value.


## 1. Introduction

A combination of high strength properties and good wear resistance together with adequate fracture toughness makes cermets attractive for applications such as high-speed machining. However, these applications often involve high steady stresses coupled with superimposed vibratory stresses, a combination can result in fatigue failure. Therefore the fatigue characteristics of cermets at high $R$ ratios are of interest ($R$ is the ratio of the minimum to the maximum stress in a fatigue cycle). However there is a limited amount of information available about the fatigue behavior of cermets and the closely-related cemented carbides in the literature. For example, Kitsunai *et a1.* [1] found in a failure analysis that fracture occurred in a cemented carbide when the stress intensity factor associated with a fatigue crack reached the value of the fracture toughness. Sato *et al.* [2] examined the influence of particle size and binder content on compressive fatigue strength of cemented carbides, and Ishihara *et al.* [3–7] investigated thermal-shock-induced fatigue crack growth behavior in cermets and cemented carbides. The present study was undertaken in order to provide additional information about the fatigue crack growth process in cermets. In this study fatigue crack growth behavior as a function of the $R$ value was investigated in a modern, complex cermet which was produced by the Nachi-Fujikoshi Corporation of Toyama, Japan.

## 2. Specimens and tests

### 2.1. Specimens

The chemical composition of the TiCN cermet used in the test program is given in Table I. The cermet contained 78 w/o particles of 0.9 $\mu$m average diameter, and 22 w/o binder phase. During the processing of the cermet, the powders were degreased, pressed, pre-baked, formed into specimen shape and baked again. The specimens were rectangular bars, 8 mm in width, 4 mm in depth and 25 mm in length. The mechanical properties of the cermet are listed in Table II. Prior to fatigue testing a transverse, 250 $\mu$m long, crack in the center of the test surface was created by making a Vickers hardness indentation at a load of 147 N. To facilitate the observation of fatigue cracks as well as to minimize any residual stresses that may have been induced by the indentation process, 40 $\mu$m were removed from the specimen test surface with emery papers and diamond paste. The resultant finish was mirror-like in quality. During the fatigue crack growth tests the crack varied in length from 250 $\mu$m to 600 $\mu$m.

### 2.2. Experimental method

The fatigue studies were carried out in laboratory air (293 K and 60–70% relative humidity) using a servo-hydraulic testing machine. The specimens were sinusoidally loaded in four-point bending at 10 Hz at stress ratios of 0.1, 0.7 and 0.9, with 2–3 specimens being used at each $R$ value. A decreasing $\Delta K$ procedure was used in the determination of the threshold level, and an increasing $\Delta K$ procedure was used at the higher fatigue crack growth rates. Fatigue crack growth tests were interrupted at periodic intervals to determine crack lengths as well as to study crack morphology by optical microscopy or by SEM. Stress intensity factors were determined using the Newman-Raju [8] expression for a surface crack in bending. This determination depends on the crack shape factor, $a/c$, where $a$ is the crack depth and $c$ is the half-crack length at the surface. A value for the $a/c$ ratio of 0.74 was used based upon the examination of the fracture surfaces after testing.

## 3. Experimental results

### 3.1. Fatigue crack growth

The rate of fatigue crack growth, d$c$/d$N$, as a function of $\Delta K$ is shown in Fig. 1 for each of the three

TABLE I Chemical composition of the material wt(%)

| Tic | TiN | WC | TaC | Mo | Ni | Co |
|---|---|---|---|---|---|---|
| 26 | 26 | 15 | 11 | 6 | 8 | 8 |

TABLE II Mechanical properties of the material

| | |
|---|---|
| Young's modulus (GPa) | 442.38 |
| Fracture toughness (MPam$^{1/2}$) | 10.8 |
| Bending strength (MPa) | 2000 |
| 0.03% Yield strength (MPa) | 1600 |
| Poisson's ratio | 0.230 |

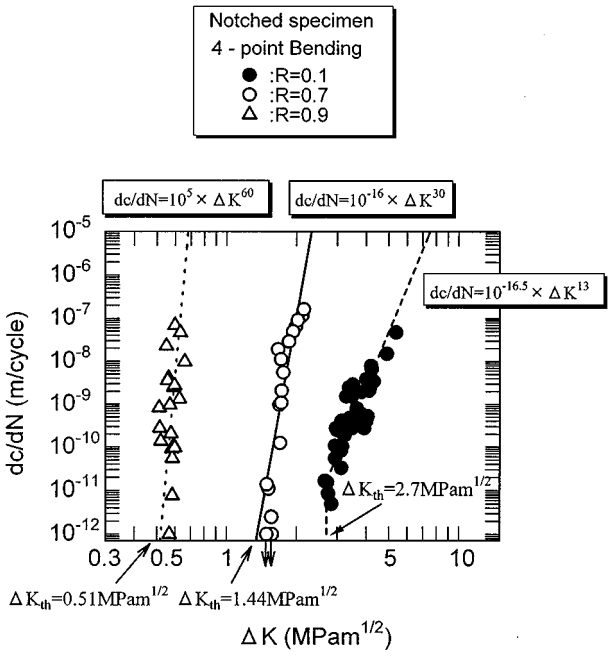


*Figure 1* Relationships between d$c$/d$N$ and stress intensity factor range, $\Delta K$, at several stress ratios.

$R$ values, 0.1, 0.7, and 0.9. The slopes of the lines through the data increase with $R$ value from 13 for $R = 0.1$ to 30 for $R = 0.7$, and to 60 for $R = 0.9$. These high slopes, particularly at the higher $R$ values indicate that the fatigue crack growth behavior of the cermet is more like that of a ceramic than a metal. From these results the rate of fatigue crack growth for each $R$ value can be approximated by

$$\text{a. For } R = 0.1, \quad \frac{\mathrm{d}c}{\mathrm{d}N} = 10^{-16.5}\Delta K^{13} \tag{1a}$$

$$\text{b. For } R = 0.7, \quad \frac{\mathrm{d}c}{\mathrm{d}N} = 10^{-16}\Delta K^{30} \tag{1b}$$

$$\text{c. For } R = 0.9, \quad \frac{\mathrm{d}c}{\mathrm{d}N} = 10^{5}\Delta K^{60} \tag{1c}$$

Further, when the data are plotted as a function of $K_{\max}$ as in Fig. 2, it is seen that at growth rates of the order of $10^{-7}$ m/cycle the rate of fatigue crack growth is more dependent upon $K_{\max}$ than upon $R$, another indication of non-metallic like behavior.

The process of fatigue crack propagation as viewed on a micro-scale was highly erratic, particularly at the

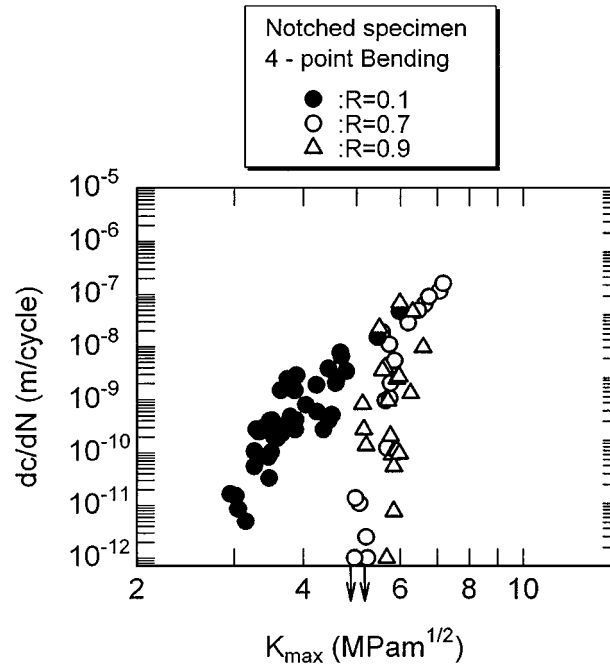


*Figure 2* Relationships between d$c$/d$N$ and the maximum stress intensity factor, $K_{\max}$, at several stress ratios.

lower growth rates under $R = 0.1$ loading, due to the interaction of the crack with particles. In fact the local growth rate could decrease by as much as three orders of magnitude below the average growth rate over a distance of 25 $\mu$m. These dramatic decreases in growth rate occurred where the crack tip was blocked by a particle. With further cycling the crack would either proceed in the binder-particle interface or perhaps appear in the binder phase beyond the particle either due to the re-initiation of the crack or to emergence of the subsurface crack. When a crack appeared beyond a particle an unbroken ligament was left behind at the surface. Until this crack-bridging ligament failed it served to reduce the rate of crack growth by reducing the crack tip opening displacement, as in the case of ceramics. At the higher crack growth rates, the arrest of a crack at a particle was less pronounced since particle cracking occurred more frequently.

Fig. 3 shows the appearance of a fatigue crack which was developed under $R = 0.1$ loading at $K_{\max}$ levels of 3.5 MPa m$^{1/2}$ and at 5.0 MPa m$^{1/2}$. The corresponding crack growth rates were $3.3 \times 10^{-9}$ and $4.2 \times 10^{-8}$ m/cycle, respectively. An examination of the fracture profile which was developed at $R = 0.1$ indicated that at the lowest crack growth rates the crack usually propagated in a zig-zag manner in the binder phase in order to bypass the particles. However, with increase in crack growth rate the crack became somewhat straighter due to the cracking of particles in the crack path. For example, due to zig-zagging, at a growth rate of $6 \times 10^{-12}$ m/cycle under $R = 0.1$ loading the actual crack path as compared to a straight path was 25% longer, whereas at a growth rate of $2 \times 10^{-7}$ m/cycle the crack path was only 15% longer. A similar decrease in total crack path with increase in crack growth rate was noted at $R = 0.9$. It was also observed that the number of cycles spent in getting a blocked crack to re-propagate

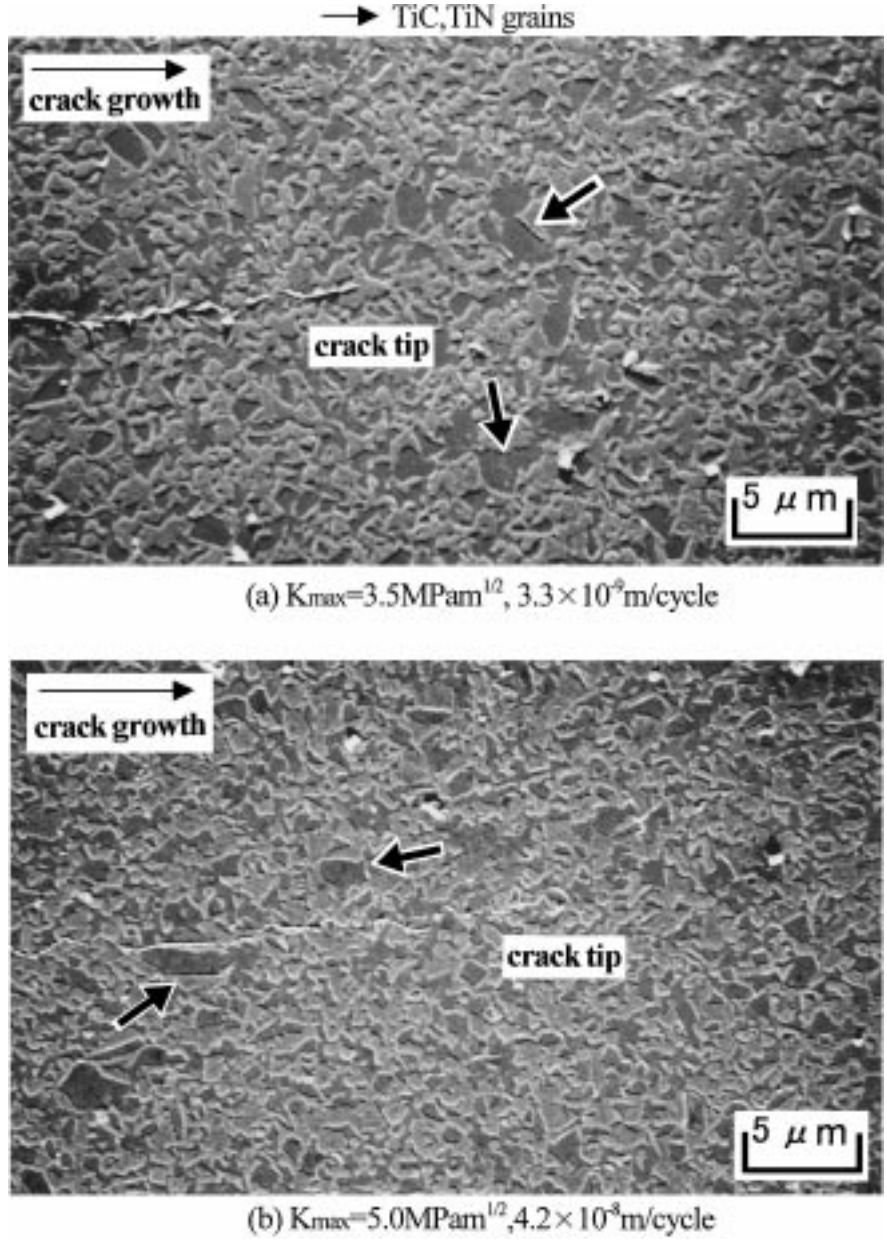


*Figure 3* Typical examples of the morphologies of a propagating crack at a stress ratio of 0.1.

increased with increase in $R$ value, and that for $R = 0.7$, an increase in $\Delta K$ with $K_{max}$ held constant, i.e., a decrease in $R$ value, resulted in a decrease in the number of cycles needed for re-propagation.

## 4. Discussion

Prior research on fatigue crack growth in particle-strengthened material has shown that the plastic zone size, $R_p$, is an important parameter affecting fatigue crack growth behavior. For example, Shang *et al.* [9] found that when a fatigue crack was blocked by a SiC particle in a SiC reinforced aluminum composite, the crack would only continue to propagate if the crack-tip plastic zone size was larger than the particle size, $d_m$. Li *et al.* [10] came to a similar conclusion in the case of $Al_2O_3$ reinforced aluminum composite. It is therefore of interest to compare this parameter with fatigue crack growth behavior of the cermet under consideration. For this purpose the monotonic plastic zone size was calculated using the following standard relation due to Irwin [11]:

$$R_p = \frac{1}{\pi}\left(\frac{K_{max}}{\sigma_{YS}}\right)^2 \quad (2)$$

where $\sigma_{YS}$ is the yield stress, which in this case is 1600 MPa. Table III lists the values of $R_p$ at threshold for each $R$ ratio, and it is seen that the Shang-Li criterion for propagation was satisfied for all $R$ values. In fact at $R = 0.9$ the plastic zone size was twice

TABLE III Plastic zone size at $K_{max,th}$

| $R$ | $K_{max,th}$ (MPa m$^{1/2}$) | $R_p$ ($\mu$m) | $R_p$/dm |
|---|---|---|---|
| 0.1 | 2.9 | 1.04 | 1.12 |
| 0.7 | 3.5 | 1.52 | 1.64 |
| 0.9 | 4.1 | 1.98 | 2.14 |

dm: diameter of hard particle.

the particle size, and this may be why at this $R$ value both particle failure at low growth rates as well as a steep slope to the d$c$/d$N$ plot were observed. In addition consideration should be given to the possibility of humidity-induced stress corrosion cracking at high $K_{max}$ values.

At threshold, the rate of fatigue crack growth was dependent upon both the mean stress and the range of stress as shown in Fig. 1. However at rates of growth above $10^{-7}$ m/cycle, the rate of growth became independent of $R$ and dependent on $K_{max}$, Fig. 2. In this range the monotonic plastic zone size was four times the particle size, and particle fracture was frequently observed at all $R$ levels.

A summary of $K_{max}$ and $\Delta K$ values as a function of $R$ is given in Fig. 4 for the threshold condition and for a growth rate of $10^{-7}$ m/cycle.

A prediction of the fatigue lifetimes of smooth specimens was made based upon the integration of Equation 1. To make the predictions it was assumed that in a smooth specimen the size of the initial defect, $2c$, was 0.006 mm, and that the critical crack size, $2c$, was 1 mm. The results of such calculations for two $R$ values are shown in Fig. 5 where they are compared with the experimental results. It is seen that the agreement between the predicted and the experimental results is quite good.

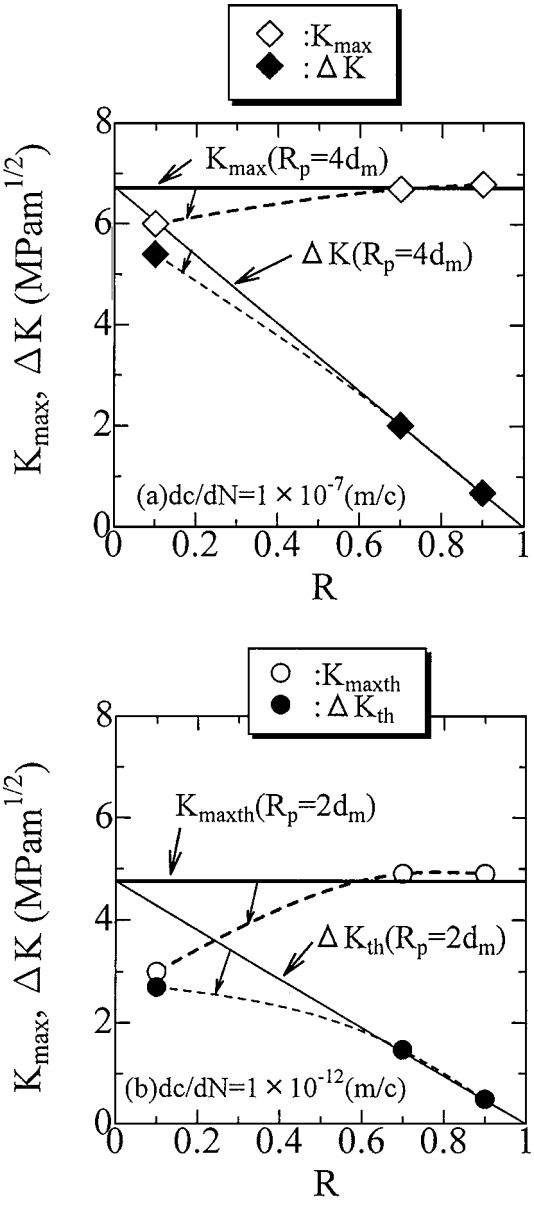


*Figure 4* Variation of $K_{max}$ and $\Delta K$ values at constant crack growth rates as a function of the stress ratio, $R$.

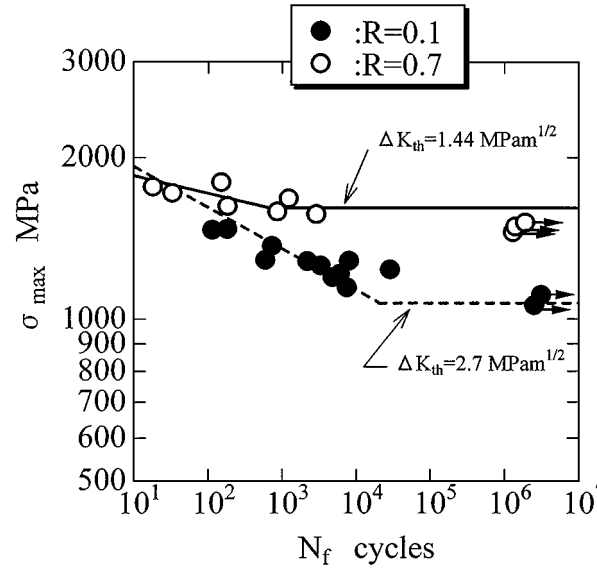


*Figure 5* A comparison of predicted (solid and dashed lines) and experimental fatigue lives at two $R$ values.

## 5. Conclusions

The effects of the stress ratio on the fatigue crack growth behavior of small cracks in a cermet were investigated. The following conclusions were reached:

1. At fatigue crack growth rates near the threshold the crack growth rate depended upon both $\Delta K$ and the $R$ value.
2. The strong dependence of the crack growth rate on $\Delta K$ was more ceramic-like than metal-like in nature.
3. At growth rates above $10^{-7}$ m/cycle the fatigue crack growth rate became $K_{max}$ dependent and independent of the $R$ value.
4. At low rates of crack growth at $R = 0.1$ the crack propagated primarily in the binder phase. At the higher $R$ values and low rates of growth the crack propagated in the binder phase as well as through the particles.
5. With increase in $K_{max}$ an increasing fraction of the crack propagation path was through the particles.
6. An excellent correlation between experimental and calculated fatigue lifetimes was obtained.


## Acknowledgement

The authors express their appreciation to Mr. K. Adachi and Mr. T. Yamauchi for assistance in doing the experiments and the discussions of the results.


## References


1. Y. KITSUNAI, Y. MAEDA and E. YOSHIHISA, *J. Mat. Sci. Japan* **40** (1991) 656.

2. K. SATO and H. HONDA, *Trans. Japan Soc. Mech. Engineers* **56A** (1996) 1378.
3. S. ISHIHARA, T. GOSHIMA, K. NOMURA and T. YOSHIMOTO, *Trans. Japan Soc. Mech. Engineers* **63A** (1997) 65.
4. S. ISHIHARA, T. GOSHIMA, K. MIYAO, T. YOSHIMOTO and S. TAKEHANA, *ibid.* **57A** (1991) 824.
5. S. ISHIHARA, T. GOSHIMA, I. NAKAYAMA and T. YOSHIMOTO, *ibid.* **62A** (1996) 1327.
6. S. ISHIHARA, T. GOSHIMA, T. YOSHIMOTO and K. NOMURA, in Proc. 6th. Int. Fatigue Congress, Fatigue '96, Berlin, 1996, p. 1633.
7. S. ISHIHARA, T. GOSHIMA, H. HARA and T. SUMI, *Japan Soc. Mech. Engineers* **63A** (1997) 1183.
8. J. C. JR. NEWMAN and I. S. RAJU, NASA technical paper, 1979, p. 1578.
9. J. K. SHANG and R. O. RITCHIE, *Acta Met.* **37** (1989) 2267.
10. C. S. LI and F. ELLYIN, *Fatigue Fract. Eng. Mater. Struct.* **18** (1995) 1299.
11. G. R. IRWIN, "Handbuch der Physik" (Springer, Berlin, 1958) p. 551.

*Received 30 June 1999*
*and accepted 2 May 2000*